RSC Advances

ROYAL SOCIETY OF CHEMISTRY

www.rsc.org/advances

RSC Advances

COMMUNICATION

Highly ordered core-shell $CoFe_2O_4$-$BiFeO_3$ nanocomposite arrays from dimension confined phase separation and their interfacial magnetoelectric coupling properties

Received 00th January 20xx,
Accepted 00th January 20xx

DOI: 10.1039/x0xx00000x

www.rsc.org/

X. L. Lu,*[a] J. W. Zhang[a], C. F. Zhang[a], J. C. Zhang[a] and Y. Hao[ab]

Different from other processes intending to induce selective nucleation in $CoFe_2O_4$-$BiFeO_3$ (CFO-BFO) immiscible multiferroic nanocomposites, a reverse way to get phase ordered CFO-BFO nanostructure was demonstrated. With dimension confinement in BFO perovskite phase, distribution of the CFO spinel phase was modulated; highly ordered core-shell CFO-BFO structure was obtained. Room temperature ferroelectricity, magnetism, and magnetoelectric coupling of as-obtained sample were characterized. These results may help to shed new light on phase ordered separation process in immiscible systems and build more heterostructures for magnetoelectric coupling applications.

As promising building blocks for low power consumption, high speed and electric field controlled spintronic devices,[1] thin film heterostructures with magnetoelectric (ME) coupling drew intensive attention recently and stimulated many breakthroughs such as electrically assisted magnetic recording,[2] multi-state tunnelling magnetoresistance,[3] reversible electrical switching of spin polarization[4] and so on. These ME heterostructures are also good model systems to study interfacial coupling of strain, charge and magnetic interactions. Recent advances in deposition technique greatly promoted the research on ME composite;[5] which makes it possible to epitaxially combine different materials horizontally as multi-layered thin film (denoted as 2-2 layout) or vertically as pillars in matrix structure (denoted as 1-3 layout).[6] In 2-2 samples, properly chosen single-crystalline substrate with matched lattice constants can be used as template to direct the growth of topping layer, giving great flexibility to vary composition and phase distribution orders in the heterostructure.[5] However, substrate induced clamping effect and critical thickness limitation dramatically hindered their practical coupling performance;[7] while in the case of 1-3 samples, interfacial strains can be maintained vertically without film thickness limitation or substrate clamping.[8] Consequently, enhanced performance was found in 1-3 systems,[2] which can provide more intrinsic insights into the interfacial interactions. But drawback of the 1-3 structure is that components are normally self-assembled during the growth, so interfaces cannot be well controlled as that in 2-2 sample. How to induce long range ordered vertical interfaces became a hot research topic with both fundamental and practical importance.[1]

Our previous results showed that in a typical 1-3 system, $CoFe_2O_4$-$BiFeO_3$ (CFO-BFO) nanocomposite, pre-deposited ordered CFO seed crystal arrays can direct nucleation of CFO nanopillars during the phase separation and bring in-plane ordering for this structure.[9] Recently, N. M. Aimon et al reported successful growth of 1-3 self-assembled nanocomposites on pre-patterned substrate,[10-12] which provided another way to control the phase distributions in 1-3 systems. Generally, with pre-introduced nucleation sites, spontaneous nucleation energy of corresponding component may be reduced and selective growth was achieved.[13] But still it is based on self-assembly process, so these nucleation centres need to match symmetry and in-plane diffusion length of the components for a successful modulation, thus only few limited layouts can be obtained from these methods.

In this communication, we reported a reverse and simple way to get ordered phase separation in CFO-BFO nanocomposites. By tuning the dimension of BFO matrix phase, distribution of CFO nanopillar phase can also be affected. As you can see in Fig. 1a, CFO nucleated spontaneously in BFO matrix; where it diffused freely and merged into many single crystalline pillars with random size and ordering as revealed by the field emission scanning electron microscopy (FE-SEM) top view image. If ordered arrays of CFO nanodots with proper symmetry and spacing were introduced to the system, CFO will then prefer to nucleate on these seeds, leading to a nanocomposite with ordered distribution and uniform size as shown in Fig. 1b. And when the in-plane dimension of BFO matrix was confined within 400 nm (comparable with the average diffusion length of CFO phase in the system,[9, 12] CFO diffusion was certainly affected, the pillars showed much closer spacing compared to those in Fig. 1a, and some of them had already merged into elongated or even maze-like squares (Fig. 1c). In this case, when the composite dimension kept shrinking down, more pillars can merge and get connected with each other, and the whole composite structure will be altered.

[a] State Key Discipline Laboratory of Wide Band Gap Semiconductor Technology, School of Microelectronics, Xidian University, 710071 Xi'an, China E-mail: xllu@live.cn
[b] School of Advanced Materials and Nanotechnology, Xidian University, 710071 Xi'an, China.

† Electronic Supplementary Information (ESI) available: [details of any supplementary information available should be included here]. See DOI: 10.1039/x0xx00000x

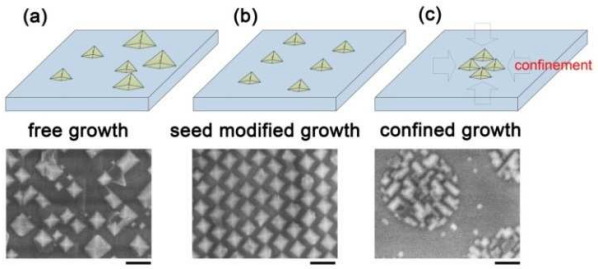

Fig. 1 Schematic and FE-SEM top view images of (a) self-assembled, (b) seed layer induced selective growth and (c) dimension confined growth of CFO-BFO nanocomposites. Scale bars are 100 nm.

Now the problem is how to induce effective and controllable confinement on this CFO-BFO nanocomposite. An anodic aluminium oxide (AAO) stencil assisted pulsed laser deposition (PLD) technique was used to grow the composites with different dimensions. AAO assisted PLD has been proven to be an efficient way for epitaxial growth of ordered structures such as $Pb(Zr_{0.2}Ti_{0.8})O_3$ nanoislands,[14] $BaTiO_3/CoFe_2O_4$ multi-layered nanodots[15, 16] and so on. So the components were deposited through AAO stencil onto $SrTiO_3$ (STO) (001) substrate. After stencil lifting off, discrete nanoislands were obtained as schematically shown in Figs. 2a and 2b. More fabrication details can be found in the support information.

All the growth condition was kept the same as that of the sample shown in Fig. 1a. Three different AAO stencils (two-step anodized at 195 V in H_3PO_4, 40 V in $H_2C_2O_4$ and 25 V in H_2SO_4) were used in the deposition. The AAO stencils showed well defined hexagonal porous structure with diameters around 350 nm in phosphoric acid AAO (denoted as Ph-AAO, Fig. 2c), 60 nm in oxalic acid AAO (denoted as Ox-AAO, Fig. S1) and 40 nm in sulphuric acid AAO (denoted as Su-AAO, Fig. S2). These ordered hexagonal patterns were successfully transferred to the composites, and highly ordered CFO-BFO nanocomposite islands with different dimensions were obtained. In Ph-AAO derived nanoislands (Fig. 2d) there are many rectangular-shaped nanodots with clear facets indicating they might be the top side of single crystalline CFO pillars. These pillars are very close to each other, some of them had already merged into maze structure, which is similar to the sample shown in Fig. 1c.

When Ox-AAO stencil (dimension around 60 nm) induced more confinement to the system, unexpectedly, only one core like nanorod can be found in the centre of each BFO island (Figs. 2e and 2f). Based on the analysis above, the core part should be CFO pillars inside BFO phase, but unlike those with clear facets in normal sample, most of the CFO pillars from Ox-AAO showed dome like shape, only very few of them showed pyramid like facet as indicated by a close-up image in Fig. 2f. This reminds us another typical 1-3 nanocomposite $CoFe_2O_4$-$BaTiO_3$ (CFO-BTO) system, where CFO separated from BTO matrix and formed round shape nanopillars with very small diameters at 750 ^{o}C.[17] Further increasing substrate temperature will increase the diameter of CFO nanopillars, which eventually showed pyramidal facets over 900 ^{o}C.[18] So in our case, the shape variation of CFO pillars might also be related to a diffusion barrier dominated process.[19]

Since the growth was normally composed of nucleation and merging process.[20] As high substrate temperature enhances the diffusion, more CFO crystal nuclei can merge into big and full crystals; on the other hand insufficient diffusion may localize CFO nucleation and lead to CFO crystals with small size. From this point of view, in Ox-AAO derived sample, when diffusion of CFO phase was suppressed by the dimension confinement, these localized CFO nuclei with very close distance can only merge with each other into one small pillar within BFO matrix; this could lead to the core-shell like heterostructures. Different composite structure was also found in Su-AAO derived sample (dimension around 40 nm), it is hard to tell CFO pillars from BFO matrix in surface topography (Fig. 3g). But if one checked very carefully, still there was slight contrast difference between the central and marginal parts in FE-SEM image, indicating different responses from CFO and BFO phase under the incident electron beam. Similar to CFO-BTO system mentioned above, additional post annealing at 800 ^{o}C led to clearly separated core-shell heterostructures as shown in Fig. 2h. This result confirmed the assumption that dimension confinement can affect CFO diffusion in 1-3 system and induce a modulation to both distribution and morphology of the nanocomposite. With this method, highly ordered core-shell heterostructure arrays were successfully fabricated.

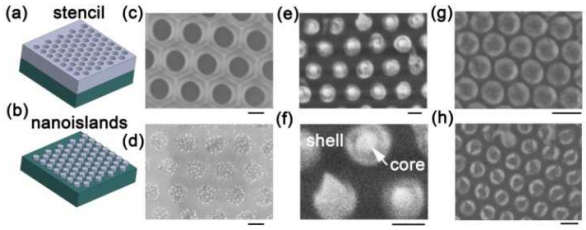

Fig. 2 (a) and (b) Schematic diagrams of AAO stencil assisted growth of ordered nanoisland arrays; (c) and (d) FE-SEM top view images of Ph-AAO stencil and as obtained CFO-BFO nanoislands, scale bars are 300 nm; (e) and (f) FE-SEM images of Ox-AAO derived highly ordered core-shell CFO-BFO nanocomposites, scale bars are 50 nm; (g) and (h) FE-SEM images of Su-AAO derived as obtained and post annealed CFO-BFO nanocomposites, scale bars are 50 nm.

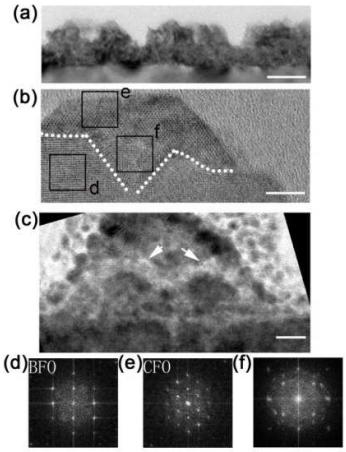

Fig. 3 (a) TEM cross section image of Ox-AAO derived CFO-BFO nanoislands, scale bar is 30 nm; HRTEM images of crystal lattices in (b) Ox-AAO derived and (c) Su-AAO derived CFO-BFO nanocomposites, scale bars are 5 nm; (d), (e) and (f) FFT images of selected areas as marked by corresponding frames in Fig. 3b.

These interesting samples had provided a bottom up chance to study phase separation and interface evolution in immiscible nanocomposite. High resolution transmission electron microscopy (HRTEM) was then used to get more structure details in as obtained core-shell islands. Fig. 3a is an overview of cross sectioned Ox-AAO derived nanoislands, in accordance with top view image in Fig. 2e, some bump like structure can be found inside these nanoislands. A close-up image (Fig. 3b) clearly shows different crystal lattices with inverted triangular interfaces (as noted by dash lines in Fig. 3b). According to fabrication process and selected area Fast Fourier Transform (FFT) image (Figs. 3d-3f), the core part should be CFO phase and shell part should be BFO matrix, while there is an intermixed region (as indicated in box F in Fig. 3b) between two phases. From the FFT analysis (Fig. 3f), it could be a mixture of BFO matrix and many tiny CFO nanocrystals. While in the result of Su-AAO derived composite island, instead of clear CFO and BFO lattices with sharp interface (like that in Fig. 3b), mixed phase of tiny nanocrystals were found in Fig. 3c. Insufficient phase diffusion might hinder the forming of full and uniform CFO crystals in BFO matrix, but still one can find a trend of diffusing and merging process in these CFO particles (as marked by arrows in Fig. 3c).

Together with these HRTEM results and FE-SEM morphology evolutions, the confined phase separation process in these core-shell nanocomposites can be preliminarily proposed as following: at early forming stage of growth, CFO phase transport was restricted due to the dimension confinement, only part of CFO nuclei within the same single AAO channel can merge and grew bigger in the following stage; some of them stay very small size due to limited diffusion like a super saturated solid solution.[20] More dimension confinement might lead to more tiny dispersive CFO nanocrystals and less single crystalline pillars in the matrix. The dimension confining altered the phase separation and induced a modulation to both distribution and morphology of the output composite. With this simple yet effective method, ordered core-shell 1-3 nanocomposite can be then fabricated, providing more functional heterostructures with tuneable interfaces for potential coupling applications.

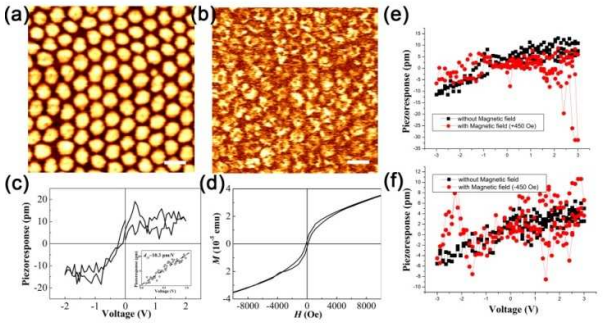

Fig. 4 (a) Topography and (b) VPFM images of Ox-AAO derived CFO-BFO nanoislands; corresponding (c) P-V and (d) M-H curves; (e) and (f) steady magnetic field induced piezoresponse change of as-prepared sample. Scale bars in (a) and (b) are 100 nm.

Besides the structure analysis above, heterointerfaces derived properties such as strain mediated ME coupling is more attractive in as obtained new nanocomposites. Strong ME coupling was already found in self-assembled CFO-BFO system, which enabled an electrical field induced perpendicular magnetization reversal at ambient conditions.[2] In our case, substrate clamping effect to BFO matrix can be reduced with its small aspect ratio (in-plane dimension to out-of-plane dimension),[21] which provides a chance to investigate intrinsic details of interfacial ME coupling of individual 1-3 nanocomposite. Therefore, piezoresponse force microscopy (PFM) was used to check local ferroelectric properties of Ox-AAO derived CFO-BFO core-shell nanoislands at room temperature. In topography image, all these islands look quite similar (Fig. 4a) while vertical PFM (VPFM) images show clear differences. The central part of each island shows weaker piezoresponse signal compared to the marginal area, leaving bright ring pattern in VPFM image (Fig. 4b). According to structure analysis above, the central parts of these islands were CFO nanopillars which certainly should not show piezoresponse, and the ring patterns in PFM image clearly indicate BFO areas. Piezoresponse vs bias Voltage (P-V loop) measurements was also checked on a randomly chosen core-shell nanoisland, which shows clear ferroelectricity at room temperature (Fig. 4c). An out-of-plane piezoelectric coefficient (d_{33}) around 10.3 pm/V were estimated from the measurement (as shown in the inset of Fig. 4c), which is lower than that of BFO thin film around the same thickness.[22] This may be related to different BFO strain state in this isolated clamping free core-shell nanoisland. And with Superconducting Quantum Interference Device (SQUID) measurement, room temperature ferromagnetic properties were also checked, as shown in Fig. 4d, Magnetization (M) vs out of plane external field (H) curve shows clear hysteresis behaviour, a coercive field around 125 Oe was found.

Since ferroelectricity and ferromagnetism were all found in these heterostructures as expected, their interaction i.e. the ME coupling effect should be more interesting. Detailed study is still underway; some preliminary data did show some interesting signals. As shown in Fig. 4e, a steady magnetic field (M field, generated by a permanent magnet) around 450 Oe (higher than the coercive field ~ 125 Oe) was firstly applied along c-axis of as-prepared sample; local piezoresponse changed correspondingly, and there was a clear increasing of piezoresponse above saturation bias around 2V. As we all know that ferroelectric BFO is highly sensitive to epitaxial strains, M field induced magnetostrictive strain in CFO can be transferred to BFO and change its piezoelectric properties. In this case, we removed external M field and checked P-V loop again at the same spot, the curve turned back to normal value (Fig. 4f); and if M field in opposite direction i.e. - 450 Oe was applied, the corresponding piezoresponse increase showed up again. Although present data was still noisy and weak, but the M filed induced piezoresponse change is quite clear and reproducible. So it is reasonable to attribute this change to strain mediated ME coupling in our CFO-BFO heterostructures which certainly deserves further investigations.

Our results had demonstrated the possibility to induce tuneable phase distribution in immiscible nanocomposite with a simple yet effective dimension confined process. Room temperature multiferroic CFO-BFO core-shell nanoisland arrays were successfully obtained. It may provide a bottom up chance to study the phase separation process in 1-3 spinel-perovskite system and help to develop interface coupling derived multi-functional properties for magnetoelectric coupling applications.

Acknowledgements

The authors acknowledge the support of National Natural Science Foundation of China (Grant 51202176) and Fundamental Research Funds for the Central Universities (Grant K5051325001).

Notes and references

1. R. Ramesh and N. A. Spaldin, *Nature Materials*, 2007, **6**, 21-29.
2. F. Zavaliche, T. Zhao, H. Zheng, F. Straub, M. P. Cruz, P. L. Yang, D. Hao and R. Ramesh, *Nano Letters*, 2007, **7**, 1586-1590.
3. Y. W. Yin, J. D. Burton, Y. M. Kim, A. Y. Borisevich, S. J. Pennycook, S. M. Yang, T. W. Noh, A. Gruverman, X. G. Li, E. Y. Tsymbal and Q. Li, *Nature Materials*, 2013, **12**, 397-402.
4. D. Pantel, S. Goetze, D. Hesse and M. Alexe, *Nature Materials*, 2012, **11**, 289-293.
5. D. G. Schlom, L.-Q. Chen, X. Pan, A. Schmehl and M. A. Zurbuchen, *Journal of the American Ceramic Society*, 2008, **91**, 2429-2454.
6. C.-W. Nan, M. I. Bichurin, S. Dong, D. Viehland and G. Srinivasan, *Journal of Applied Physics*, 2008, **103**, 031101.
7. P. Zhao, Z. L. Zhao, D. Hunter, R. Suchoski, C. Gao, S. Mathews, M. Wuttig and I. Takeuchi, *Applied Physics Letters*, 2009, **94**, 243507.
8. S. A. Harrington, J. Y. Zhai, S. Denev, V. Gopalan, H. Y. Wang, Z. X. Bi, S. A. T. Redfern, S. H. Baek, C. W. Bark, C. B. Eom, Q. X. Jia, M. E. Vickers and J. L. MacManus-Driscoll, *Nature Nanotechnology*, 2011, **6**, 491-495.
9. S. M. Stratulat, X. L. Lu, A. Morelli, D. Hesse, W. Erfurth and M. Alexe, *Nano Letters*, 2013, **13**, 3884-3889.
10. D. H. Kim, N. M. Aimon, X. Y. Sun and C. A. Ross, *Advanced Functional Materials*, 2014, **24**, 2334-2342.
11. N. M. Aimon, H. K. Choi, X. Y. Sun, D. H. Kim and C. A. Ross, *Advanced Materials*, 2014, **26**, 3063-3067.
12. N. M. Aimon, D. H. Kim, X. Sun and C. A. Ross, *ACS Applied Materials & Interfaces*, 2015, **7**, 2263-2268.
13. R. Comes, H. Liu, M. Kholchov, R. Kasica, J. Lu and S. A. Wolf, *Nano Letters*, 2012, **12**, 2367-2373.
14. W. Lee, H. Han, A. Lotnyk, M. A. Schubert, S. Senz, M. Alexe, D. Hesse, S. Baik and U. Gosele, *Nature Nanotechnology*, 2008, **3**, 402-407.
15. X. L. Lu, Y. Kim, S. Goetze, X. Li, S. Dong, P. Werner, M. Alexe and D. Hesse, *Nano Letters*, 2011, **11**, 3202-3206.
16. X. L. Lu, S. Dong, X. Li, M. Alexe, D. Hesse and Y. Hao, *Applied Physics Letters*, 2012, **101**, 222902.
17. H. Zheng, J. Wang, L. Mohaddes-Ardabili, M. Wuttig, L. Salamanca-Riba, D. G. Schlom and R. Ramesh, *Applied Physics Letters*, 2004, **85**, 2035-2037.
18. L. Yan, F. Bai, J. Li and D. Viehland, *Philosophical Magazine*, 2010, **90**, 103-111.
19. H. M. Zheng, F. Straub, Q. Zhan, P. L. Yang, W. K. Hsieh, F. Zavaliche, Y. H. Chu, U. Dahmen and R. Ramesh, Advanced Materials, 2006, **18**, 2747-2752.
20. D. P. Norton, *Materials Science & Engineering R-Reports*, 2004, **43**, 139-247.
21. J. Zhang, H. Fu, W. Lu, J. Dai and H. L. W. Chan, *Nanoscale*, 2013, **5**, 6747-6753.
22. J. Wang, J. B. Neaton, H. Zheng, V. Nagarajan, S. B. Ogale, B. Liu, D. Viehland, V. Vaithyanathan, D. G. Schlom, U. V. Waghmare, N. A. Spaldin, K. M. Rabe, M. Wuttig and R. Ramesh, *Science*, 2003, **299**, 1719-1722.

Table of Contents Graphics

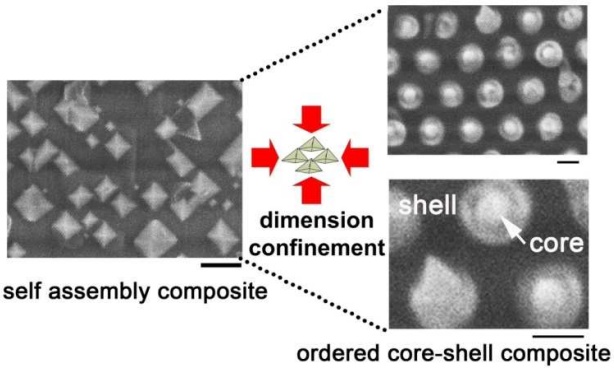

With dimension confinement, highly ordered core-shell $CoFe_2O_4$-$BiFeO_3$ nanocomposite arrays were obtained from the self-assembly phase separation.